



Trade Science Inc.

March 2010

ISSN : 0974 - 746X

Volume 5 Issue 1

Inorganic CHEMISTRY

An Indian Journal

Full Paper

ICAIJ, 5(1), 2010 [31-45]

Spectroscopic and structural studies of some transition metal complexes of a synthetic ligands derived from 4-acetylpyridine

Moamen S.Refat^{1,2*}, Ibrahim M.El-Deen³, Hassan K.Ibrahim³, Jehan A.Hasanen³

¹Department of Chemistry, Faculty of Science, Port Said, Suez Canal University, Port Said, (EGYPT)

²Department of Chemistry, Faculty of Science, Taif University, 888 Taif, Kingdom, (SAUDIARABIA)

³Department of Chemistry, Faculty of Science, Ismailia, Suez Canal University, Ismailia, (EGYPT)

E-mail : msrefat@yahoo.com

Received: 9th January, 2010 ; Accepted: 19th January, 2010

ABSTRACT

Co(II), Ni(II) and Cu(II) complexes with novel heterocyclic ligands derived from 4-acetylpyridine with thiosemicarbazide were synthesized and characterized by elemental analysis, molar conductivity, spectral methods (mid infrared, ¹H-NMR, mass and UV/vis spectra) and simultaneous thermal analysis (TG and DTG) techniques. The molar conductance measurements proved that all complexes are electrolytes compared with their ligands. The IR spectra of the two ligands and their complexes are used to identify the type of bonding. The kinetic thermodynamic parameters such as: E*, ΔH*, ΔS* and ΔG* are estimated from the DTG curves. The free ligands and their complexes have been studied for their possible biological activity (antibacterial and antifungal). © 2010 Trade Science Inc. - INDIA

KEYWORDS

4-acetylpyridine;
Infrared spectra;
Thermal analysis;
¹H-NMR spectra;
Microbiological screening.

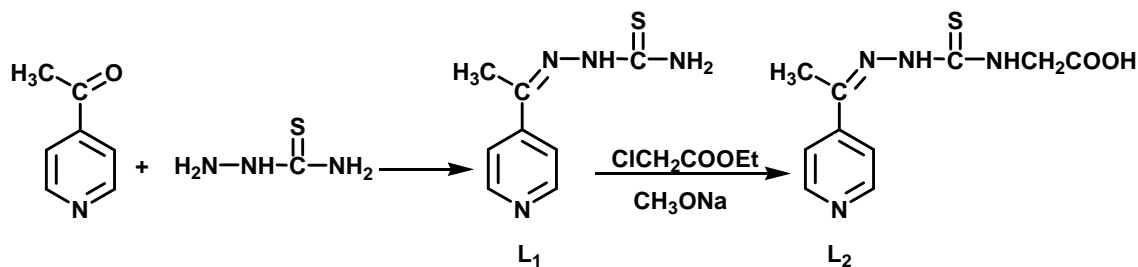
INTRODUCTION

Metal complexes containing 4-pyridine moiety such as 1-(pyridine-4-yl) ethylidene) hydrazinecarbothioamide and 1-(pyridine-4-yl) ethylidene amino) 2-thioxoimidazolidin derivatives have aroused considerable interest in view of their industrial and biological importance.

Many of these compounds possess a wide spec-

trum of medicinal properties, including activity against tuberculosis, leprosy, and bacterial and viral infections. They have also been found to be active against influenza, protozoa, smallpox, psoriasis, rheumatism, trypanosomiasis, coccidiosis, malaria and certain kinds of tumors and have been suggested as possible pesticides and fungicides. Their activity has frequently been thought to be due to their ability to chelate trace metals^[1-5].

The present study discuss the synthesis, spectro-



Full Paper

scopic characterization and biological screening of heterocyclic ligands derived from 4-acetylpyridine with thio- semicarbazide towards Co(II), Ni(II) and Cu(II) ions.

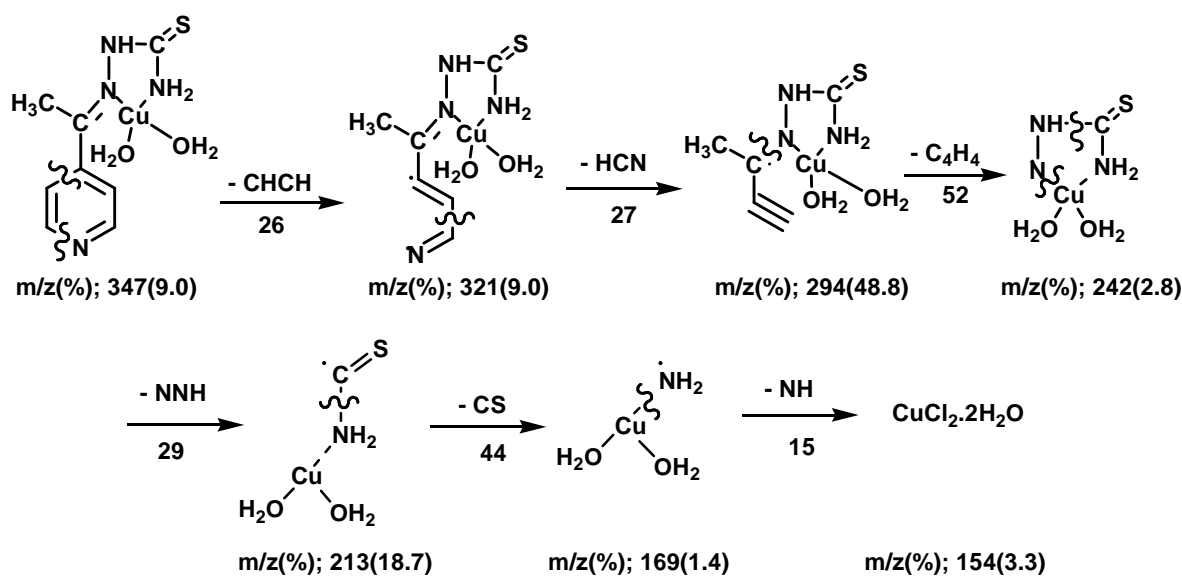
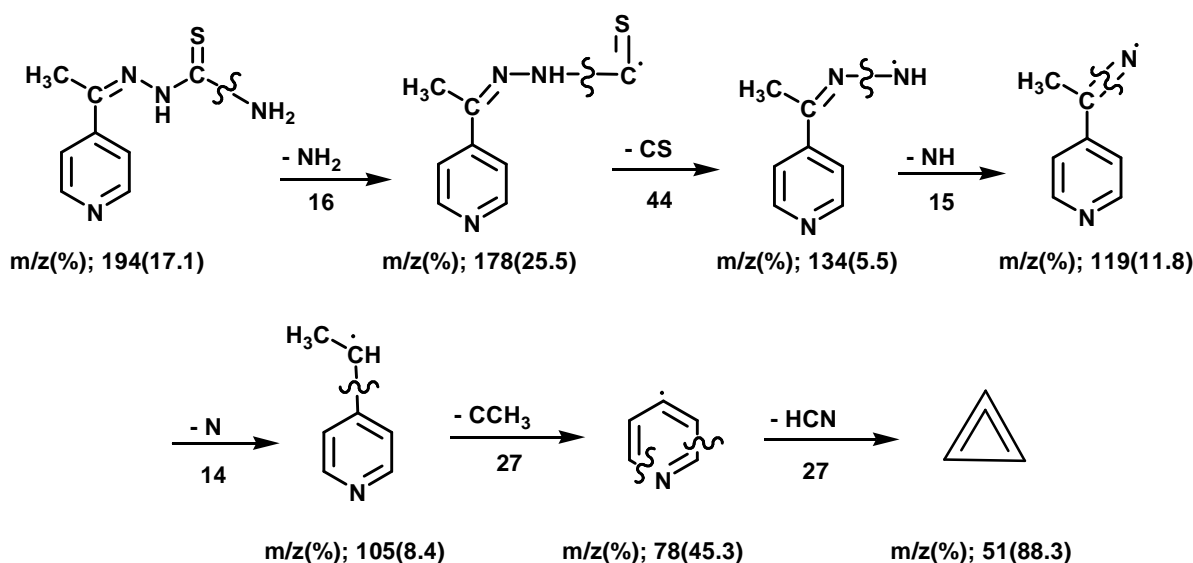
EXPERIMENTAL

Materials and instrumentation

All chemicals were reagent grade and were used without further purification. 4-acetylpyridine, thiosemicarbazide and chloro acetic acid were purchased from Fluka Chemical Co., $\text{CoCl}_2 \cdot 6\text{H}_2\text{O}$, $\text{NiCl}_2 \cdot 6\text{H}_2\text{O}$ and $\text{CuCl}_2 \cdot 2\text{H}_2\text{O}$ from (Merck Co.).

Carbon, hydrogen and nitrogen contents were determined using a Perkin-Elmer CHN 2400 in the Micro-analytical Unit at the Faculty of Science, Cairo University, Egypt. The metal content was found gravimetrically by converting the compounds into their corresponding oxides.

IR spectra were recorded on Bruker FTIR Spectrophotometer ($4000\text{--}400\text{cm}^{-1}$) in KBr pellets. The UV-vis, spectra were determined in the DMSO solvent with concentration ($1.0 \times 10^{-3}\text{ M}$) for the free ligands and their complexes using Jenway 6405 Spectrophotometer with 1 cm quartz cell, in the range 200-800nm. Molar conductivities of freshly prepared $1.0 \times 10^{-3}\text{ mol/dm}^{-3}$



DMSO solutions were measured using Jenway 4010 conductivity meter.

¹H-NMR spectrum of the two ligands (L₁ and L₂), Ni-L₁ and Cu-L₂ complexes were recorded on Varian Gemini 200 MHz spectrometer using DMSO-d₆ as solvent and TMS as an internal reference. The purity of the two ligands, L₁-Cu and L₂-Co were checked from mass spectra at 70eV by using AEI MS 30 Mass spectrometer. Thermogravimetric analysis (TGA and DTG) were carried out in dynamic nitrogen atmosphere (30ml/min) with a heating rate of 10 C/min using a Schimadzu TGA-50H thermal analyzer.

Synthesis of L₁ and L₂

[(2-(1-pyridin-4-yl) ethylidene)-4-hydrazine-carbothioamide] [L₁]

A mixture of 4-acetylpyridine (12.1gm, 0.1 mole), thiosemicarbazide (12gm, 0.13 mole) and methanol (100ml) was heated under reflux for 2 hr. after cooling the precipitate was filtered off, washed with methanol, crystallized from methanol to give white crystals.

[(2-(2-(1-(pyridine-4-yl) ethylidene) hydrazine-carbothioamido) acetic acid] [L₂]

A mixture of (L₁) (0.1 mole), and chloroethylacetate (0.1mole) was added to solution of sodium methoxide (100ml) and heated under reflux for 2hr. after cooling the precipitate was filtered off, crystallized from methanol to give yellow crystals.

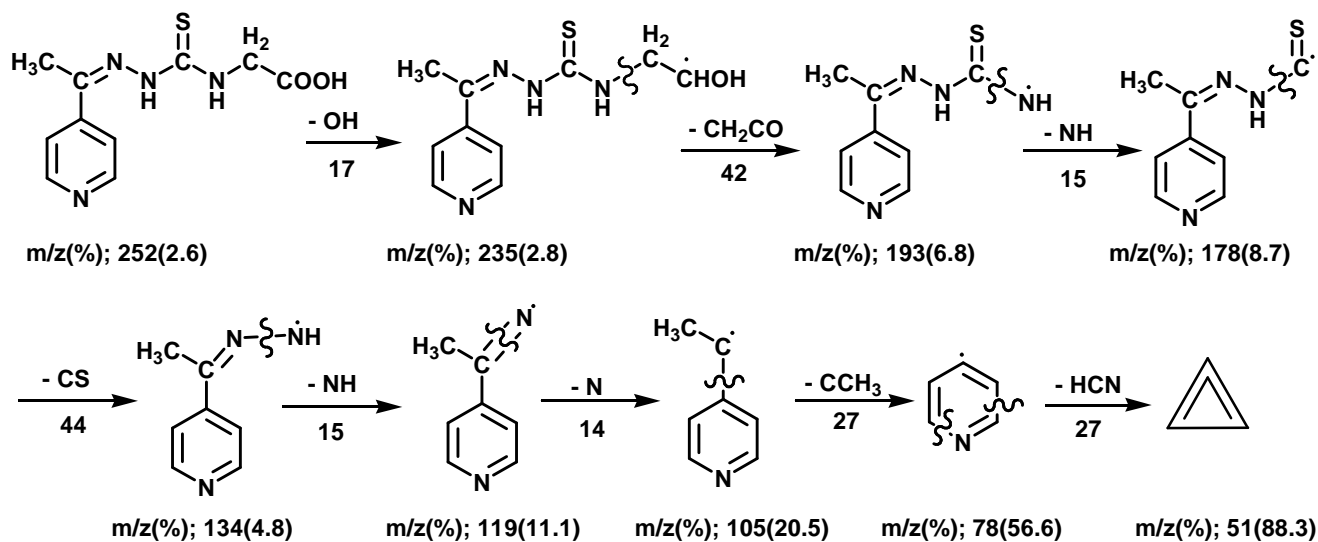
Synthesis of the complexes

A general method is: the desired weight of the free ligands was dissolved in 30 ml methanol and the solution was adjusted to pH 7.0 by addition of methanolic solution of ammonium hydroxide. The metal salts were dissolved in 20 ml of methanol and then the prepared solutions were slowly added to the solution of the ligand under magnetic stirring. After heating for about 1 h, the obtained precipitates were filtered off, wash with hot methanol and dried at 60°C.

Microbiological screening

For these investigations the hole well method was applied. The investigated isolates of bacteria were seeded in tubes with nutrient broth (NB). The seeded NB (1cm³) was homogenized in the tubes with 9cm³ of melted (45°C) nutrient agar (NA). The homogeneous suspensions were poured into Petri dishes. The holes (diameter 4 mm) were done in the cool medium. After cooling in these holes, 2 × 10⁻³ dm³ of the investigated compounds were applied using a micropipette. After incubation for 24 h in a thermostat at 25-27°C, the inhibition (sterile) zone diameters (including disc) were measured and expressed mm. An inhibition zone diameter over 7mm indicates that the tested compound is active against the bacteria under investigation.

The antibacterial activities of the investigated compounds were tested against *Bacillus Subtilis*, *Streptococcus Penumonia*, *Staphylococcus aureus* (as Gram Positive Bacteria), *Escherichia Coli* and *Pesudomonas*



Scheme 3 : Fragmentation pattern of L₂

Full Paper

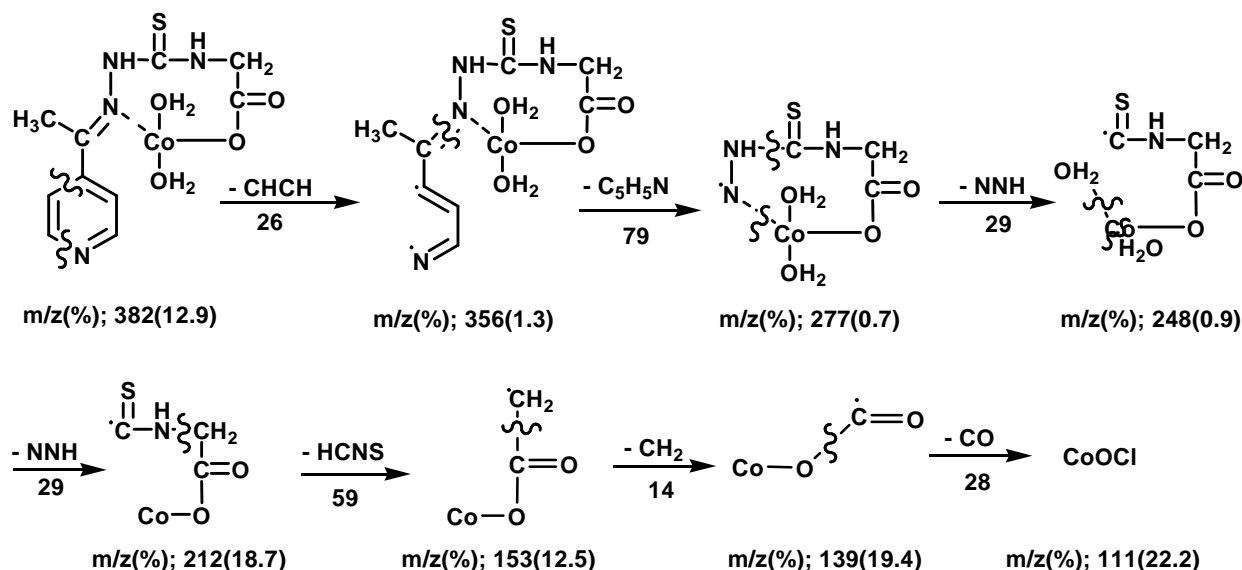
Scheme 4 : Fragmentation pattern of $[\text{CoL}_2(\text{H}_2\text{O})_2]\text{Cl}$ (IV)

TABLE 1 : Elemental analyses and physical data of the two ligands and their complexes (I-VI)

Compounds	Mwt.	mp/ $^{\circ}\text{C}$	color	Content ((calculated) found)				Δm μs
				% C	% H	% N	%M	
$\text{L}_1(\text{C}_8\text{H}_{10}\text{N}_4\text{S})$	194.00	230	Colorless	(49.48) 49.21	(5.15) 4.08	(28.86) 28.39	-	39.21
$\text{L}_2(\text{C}_{10}\text{H}_{12}\text{N}_4\text{O}_2\text{S})$	252.00	215	Yellow	(47.61) 46.89	(4.76) 4.61	(22.20) 21.79	-	22.33
$[\text{CoL}_1(\text{H}_2\text{O})_2](\text{Cl})_2$ (I, $\text{C}_8\text{H}_{14}\text{N}_4\text{O}_2\text{SCl}_2\text{Co}$)	359.93	>350	Orange	(26.67) 26.49	(3.89) 3.78	(15.56) 16.01	(16.37) 16.59	245.20
$[\text{NiL}_1(\text{H}_2\text{O})_2](\text{Cl})_2 \cdot 2\text{H}_2\text{O}$ (II, $\text{C}_8\text{H}_{18}\text{N}_4\text{O}_4\text{SCl}_2\text{Ni}$)	395.69	>350	Green	(24.26) 24.98	(4.55) 4.99	(14.15) 14.21	(14.83) 14.61	228.30
$[\text{CuL}_1(\text{H}_2\text{O})_2](\text{Cl})_2$ (III, $\text{C}_8\text{H}_{14}\text{N}_4\text{O}_2\text{SCl}_2\text{Cu}$)	364.50	>350	Red brown	(26.34) 26.49	(3.84) 4.00	(15.36) 15.96	(17.42) 17.84	311.21
$[\text{CoL}_2(\text{H}_2\text{O})_2]\text{Cl}$ (IV, $\text{C}_{10}\text{H}_{15}\text{N}_4\text{O}_4\text{SClCo}$)	381.43	>350	Brown	(31.46) 31.08	(3.93) 4.70	(14.68) 14.19	(15.44) 15.52	114.50
$[\text{NiL}_2(\text{H}_2\text{O})_4]\text{Cl} \cdot 2\text{H}_2\text{O}$ (V, $\text{C}_{10}\text{H}_{23}\text{N}_4\text{O}_8\text{SClNi}$)	453.15	>350	Green	(26.48) 26.93	(4.36) 4.36	(12.35) 12.47	(12.95) 11.97	106.20
$[\text{CuL}_2(\text{H}_2\text{O})_4]\text{Cl}$ (VI, $\text{C}_{10}\text{H}_{19}\text{N}_4\text{O}_6\text{SClCu}$)	422.00	>350	Deep green	(28.43) 29.27	(4.50) 4.55	(13.27) 13.27	(15.04) 15.63	195.20

Sp. (as Gram Negative Bacteria) and as well as some kinds of fungi; *Aspergillus Nigraer* and *Penicillium Sp.*. In the same time with the antibacterial and antifungal investigations of the complexes, the two ligands were also tested, as well as the pure solvent. The concentration of each solution was 1.010^{-3} mol dm^3 . Commercial DMSO was employed to dissolve the tested samples.

RESULTS AND DISCUSSION

The results of the elemental analysis and some physical characteristics of the obtained compounds are given in TABLE 1.

The complexes are air-stable, hygroscopic, with higher melting points, insoluble in H_2O and most of organic solvents, but soluble in DMSO and DMF.

Condensation of 4-acetylpyridine with thiosemi-carbazide readily gives rise to the corresponding L_1 and L_2 , which was easily identified by its IR, $^1\text{H-NMR}$ and mass spectra. Bidentate complexes were obtained upon reaction between metal ions of and L_1 and L_2 ligands at 1:1 molar ratio. The ligands L_1 and L_2 on reaction with $\text{CoCl}_2 \cdot 6\text{H}_2\text{O}$, $\text{NiCl}_2 \cdot 6\text{H}_2\text{O}$ and $\text{CuCl}_2 \cdot 2\text{H}_2\text{O}$ salts, yield complexes corresponding to the general formula $[\text{CoL}_1(\text{H}_2\text{O})_2]\text{Cl}_2$ (I), $[\text{NiL}_1(\text{H}_2\text{O})_2]\text{Cl}_2 \cdot 2\text{H}_2\text{O}$ (II), $[\text{CuL}_1(\text{H}_2\text{O})_2]\text{Cl}_2$ (III), $[\text{CoL}_2(\text{H}_2\text{O})_2]\text{Cl}$ (IV),

TABLE 2 : IR frequencies (cm⁻¹) of the L₁ and L₂ and their metal complexes

Assignments	Compound							
	L ₁	L ₂	I	II	III	IV	V	VI
$\nu_{as}(\text{OH}); \text{H}_2\text{O}$	-	-	3345	3308	3360	3333	3360	3314
$\nu(\text{N-H})$	3456	3296	-	-	-	-	-	-
$\nu(\text{C-H})$ aromatic	3170	3076	-	-	-	-	-	-
$\nu(\text{COOH})$	-	1711	-	-	-	-	-	-
$\nu_{as}(\text{COO}^-)$	-	-	-	-	-	1500	1509	1542
$\nu(\text{C=N})$	1630	1632	1612	1602	1611	1609	1611	1611
$\nu(\text{M-N})$	-	-	430	451	458	432	450	493

[NiL₂(H₂O)₄]Cl.2H₂O (V), [CuL₂(H₂O)₄]Cl (VI). The newly synthesized ligands and its complexes are very stable at room temperature in the solid state. The analytical data are in a good agreement with the proposed stoichiometry of the complexes. The metal-to-ligand ratio in the Co(II), Ni(II) and Cu(II) complexes was found to be 1:1.

Molar conductivities of the metal chelates

The molar conductivity values for the complexes in DMSO solvent (1.0×10^{-3} mol) were in the range (114.30-311.60) μS . The molar conductivity measurements in the range of electrolytic nature (TABLE 1). Conductivity measurements have frequently been used in structural of metal chelates (mode of coordination) within the limits of their solubility. They provide a method of testing the degree of ionization of the complexes, the molecular ions that a complex liberates in solution (incase of presence anions outside the coordination sphere), the higher will be its molar conductivity and vice versa^[6]. It is clear from the conductivity data, compared with the values of free ligands that the complexes present seem to be electrolytes. Also the molar conductance values indicate that the anions may be exhibits outside or absent or inside the coordination sphere. This result was strongly supported with the chemical analysis (elemental analysis data) where Cl⁻ ions are detected by addition of AgNO₃ solution. Also the conductivity values for L₁ complexes are greater than that for L₂, where they have two chlorine atoms.

Infrared spectra

The main IR data of the two ligands L₁, L₂ and their complexes are summarized in TABLE 2 and IR spectra are shown in Figure 1. The presence of the broad

TABLE 3 : The electronic spectral date of the L₁ and L₂ and their metal complexes (I-VI)

Compound	λ_{max} (nm)	$\epsilon(\text{mole}^{-1} \text{cm}^{-1})$	Assignment
L ₁	220	234	$\pi-\pi^*$ trans.
	235	1788	$\pi-\pi^*$ trans.
	325	1945	$n-\pi^*$ trans.
L ₂	210	407	$\pi-\pi^*$ trans.
	220	270	$\pi-\pi^*$ trans.
	240	676	$\pi-\pi^*$ trans.
	330	1516	$n-\pi^*$ trans.
[CoL ₁ (H ₂ O)](Cl) ₂	220	3000	$\pi-\pi^*$ trans.
	235	1431	$\pi-\pi^*$ trans.
	345	1861	$n-\pi^*$ trans.
[NiL ₁ (H ₂ O) ₂](Cl) ₂ .2H ₂ O	205	3000	$\pi-\pi^*$ trans.
	215	3000	$\pi-\pi^*$ trans.
	240	1426	$\pi-\pi^*$ trans.
	335	2656	$n-\pi^*$ trans.
[CuL ₁ (H ₂ O)](Cl) ₂	210	3000	$\pi-\pi^*$ trans.
	220	595	$\pi-\pi^*$ trans.
	245	2196	$\pi-\pi^*$ trans.
	285	2377	$n-\pi^*$ trans.
	330	2977	$n-\pi^*$ trans.
[CoL ₂ (H ₂ O) ₂]Cl	350	2905	$n-\pi^*$ trans.
	235	1539	$\pi-\pi^*$ trans.
	340	2855	$n-\pi^*$ trans.
[NiL ₂ (H ₂ O) ₄]Cl.2H ₂ O	350	2719	$n-\pi^*$ trans.
	215	1054	$\pi-\pi^*$ trans.
	240	1054	$\pi-\pi^*$ trans.
	250	1054	$\pi-\pi^*$ trans.
	260	802	$\pi-\pi^*$ trans.
	285	541	$n-\pi^*$ trans.
	385	1412	$n-\pi^*$ trans.
448	440	L \rightarrow Ni C.T.	
[CuL ₂ (H ₂ O) ₄]Cl	210	1854	$\pi-\pi^*$ trans.
	235	785	$\pi-\pi^*$ trans.
	335	1091	$n-\pi^*$ trans.

water bands in the 3308-3360cm⁻¹ zone confirms the presence of water molecules in all complexes. The stretching vibration, $\nu(\text{NH})$, which appears at 3456 cm⁻¹ in the spectrum of L₁ is shifted in the spectra of its complexes, which indicate the sharing of NH₂ group in the formation of the complexes. However, the absence of the absorption band at 1711 cm⁻¹, arising from the carboxylic group (COOH) for under investigation L₂ com-

Full Paper

TABLE 4 : Thermal data of the L₁ and L₂ complexes (I-VI)

Compound	Steps	Temperature range (°C)	DTG peak (°C)	TG		Assignments
				Weight loss (%)	Calc. Found	
[CoL ₁ (H ₂ O)](Cl) ₂	1 st	25-250	150	22.82	21.85	C ₅ H ₄ N (pyridine ring)
	2 nd	250-400	300	39.19 37.99	39.28 38.87	C ₃ H ₈ N ₃ OS (organic moiety) CoCl ₂ (residue)
[NiL ₁ (H ₂ O) ₂](Cl) ₂ .2H ₂ O	1 st	25-100	75	18.19	17.83	4H ₂ O
	2 nd	100-225	175	19.72	19.86	C ₅ H ₄ N (pyridine ring)
	3 rd	225-400	315	29.32 32.77	29.52 32.79	C ₃ H ₆ N ₃ S (organic moiety) NiCl ₂ (residue)
[CuL ₁ (H ₂ O)](Cl) ₂	1 st	25-200	125	22.52	22.53	C ₅ H ₄ N (pyridine ring)
	2 nd	200-400	250	38.67 38.81	39.29 38.18	C ₃ H ₈ N ₃ OS (organic moiety) CuCl ₂ (residue)
[CoL ₂ (H ₂ O) ₂]Cl	1 st	25-100	65	9.43	9.51	2H ₂ O
	2 nd	100-400	250	61.61 28.96	60.05 30.44	C ₁₀ H ₁₁ N ₄ OS (organic moiety) CoO (residue)
[NiL ₂ (H ₂ O) ₄]Cl.2H ₂ O	1 st	25-225	65	23.83	23.51	6H ₂ O
	2 nd	225-400	250	61.61 28.96	60.05 30.44	C ₁₀ H ₁₁ N ₄ OS (organic moiety) NiO (residue)
[CuL ₂ (H ₂ O) ₄]Cl	1 st	25-150	115	12.79	12.52	3H ₂ O
	2 nd	150-400	300	59.95 27.26	59.79 27.69	C ₁₀ H ₁₃ N ₄ O ₂ S (organic moiety) CuO (residue)

TABLE 5 : Kinetic parameters using the Coats–Redfern (CR) and Horowitz–Metzger (HM) operated for the L₁ and L₂ complexes (I-VI)

Complex	Stage	Method	Parameter					r
			E (J mol ⁻¹)	A (s ⁻¹)	ΔS (J mol ⁻¹ K ⁻¹)	ΔH (J mol ⁻¹)	ΔG (J mol ⁻¹)	
I	1 st	CR	6.82 × 10 ⁴	3.87 × 10 ⁶	-1.22 × 10 ²	6.48 × 10 ⁴	1.16 × 10 ⁵	0.9954
		HM	7.39 × 10 ⁴	2.14 × 10 ⁷	-1.07 × 10 ²	7.04 × 10 ⁴	1.15 × 10 ⁵	0.9994
		average	7.10 × 10 ⁴	1.26 × 10 ⁷	-1.14 × 10 ²	6.76 × 10 ⁴	1.15 × 10 ⁵	
II	2 nd	CR	5.46 × 10 ⁴	7.09 × 10 ³	-1.75 × 10 ²	5.08 × 10 ⁴	1.32 × 10 ⁵	0.9998
		HM	6.50 × 10 ⁴	1.94 × 10 ⁵	-1.47 × 10 ²	6.11 × 10 ⁴	1.79 × 10 ⁵	0.9995
		average	5.98 × 10 ⁴	1.01 × 10 ⁵	-1.61 × 10 ²	5.59 × 10 ⁴	1.55 × 10 ⁵	
III	1 st	CR	2.04 × 10 ⁴	4.56 × 10 ¹	-2.35 × 10 ²	1.69 × 10 ⁴	1.15 × 10 ⁵	0.9923
		HM	3.78 × 10 ⁴	3.46 × 10 ²	-1.99 × 10 ²	3.44 × 10 ⁴	1.18 × 10 ⁵	0.9997
		average	2.91 × 10 ⁴	1.95 × 10 ²	-2.17 × 10 ²	2.56 × 10 ⁴	1.16 × 10 ⁵	
IV	2 nd	CR	2.84 × 10 ⁵	1.93 × 10 ²⁷	2.73 × 10 ²	2.79 × 10 ⁴	1.42 × 10 ⁵	0.9992
		HM	3.02 × 10 ⁵	7.26 × 10 ²⁹	3.22 × 10 ²	2.97 × 10 ⁴	1.35 × 10 ⁵	0.9999
		average	2.93 × 10 ⁵	3.63 × 10 ²⁹	2.97 × 10 ²	2.88 × 10 ⁴	1.38 × 10 ⁵	
V	1 st	CR	3.96 × 10 ⁴	2.83 × 10 ⁴	-2.01 × 10 ²	3.61 × 10 ⁴	1.21 × 10 ⁵	0.9630
		HM	4.74 × 10 ⁴	5.62 × 10 ³	-1.76 × 10 ²	4.39 × 10 ⁴	1.18 × 10 ⁵	0.9975
		average	4.35 × 10 ⁴	1.69 × 10 ⁴	-1.90 × 10 ²	4.00 × 10 ⁴	1.19 × 10 ⁵	
VI	1 st	CR	1.94 × 10 ⁵	2.73 × 10 ²³	2.01 × 10 ²	1.91 × 10 ⁵	1.10 × 10 ⁵	0.9956
		HM	2.01 × 10 ⁵	4.16 × 10 ²⁴	2.24 × 10 ²	1.98 × 10 ⁵	1.07 × 10 ⁵	0.9947
		average	1.97 × 10 ⁵	2.21 × 10 ²⁴	2.12 × 10 ²	1.94 × 10 ⁵	1.08 × 10 ⁵	

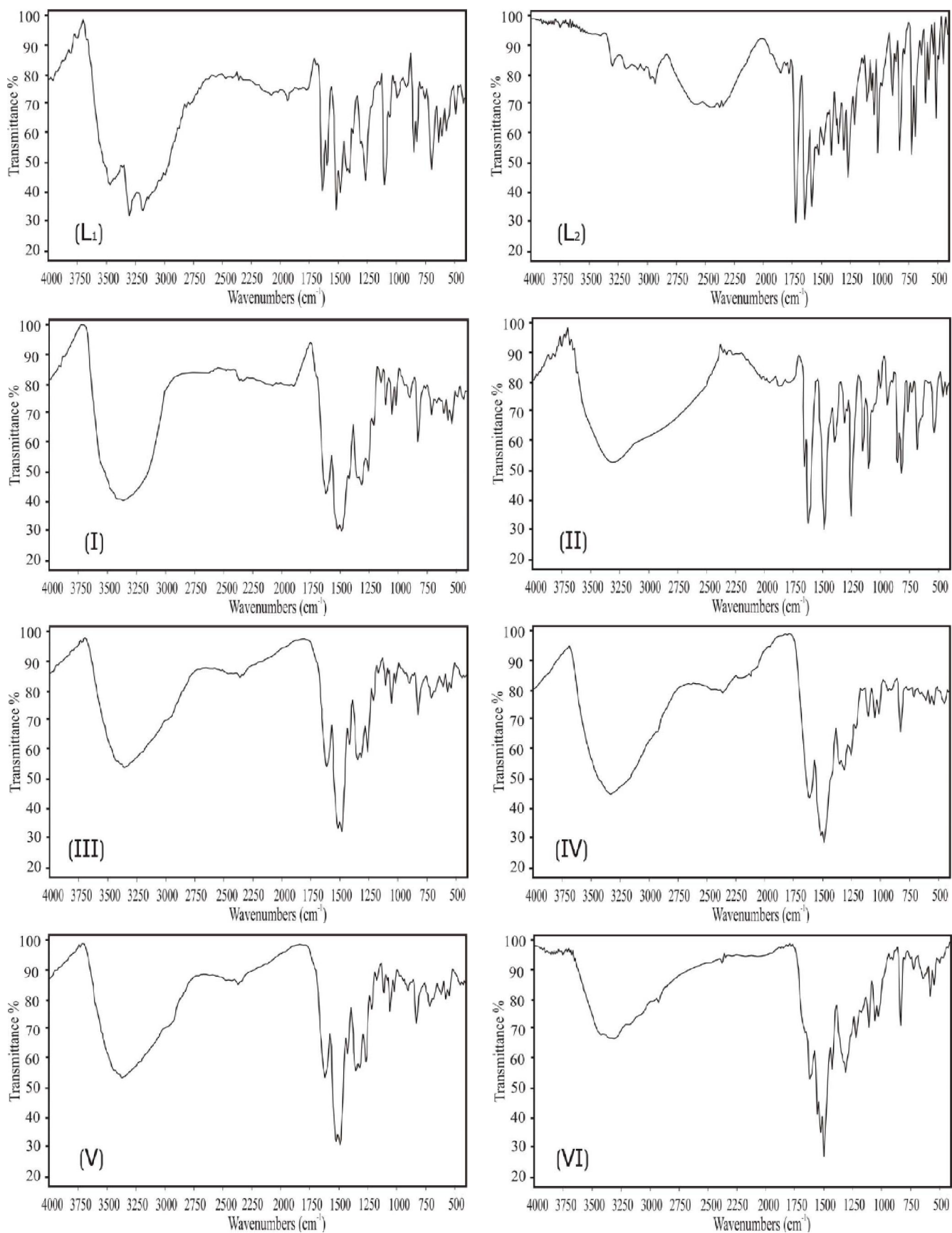
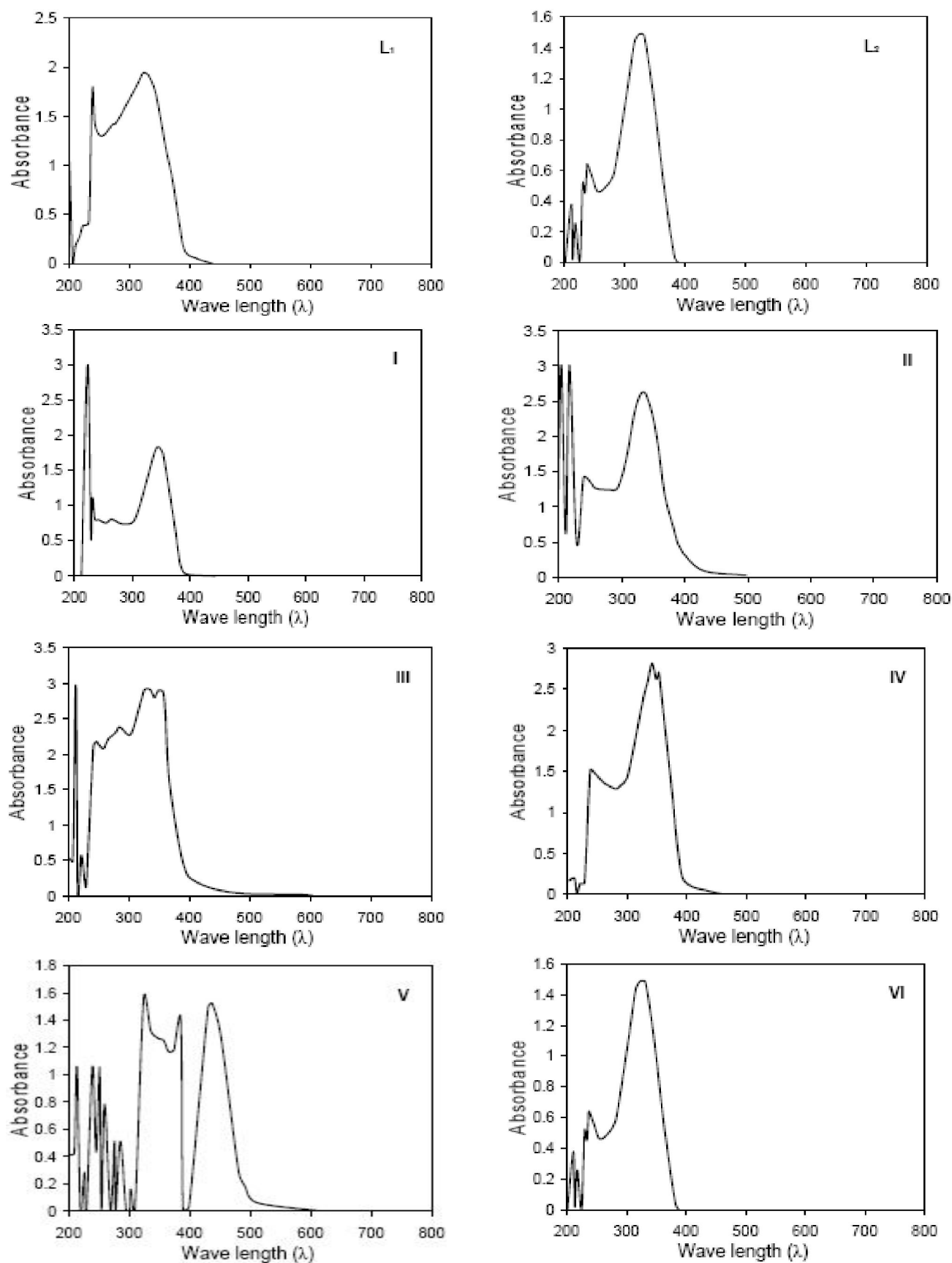


Figure 1 : The FT-IR spectra of L₁ and L₂ and their complexes (I-VI)

Full Paper

Figure 2 : The UV spectra of L_1 and L_2 and their complexes (I-VI)

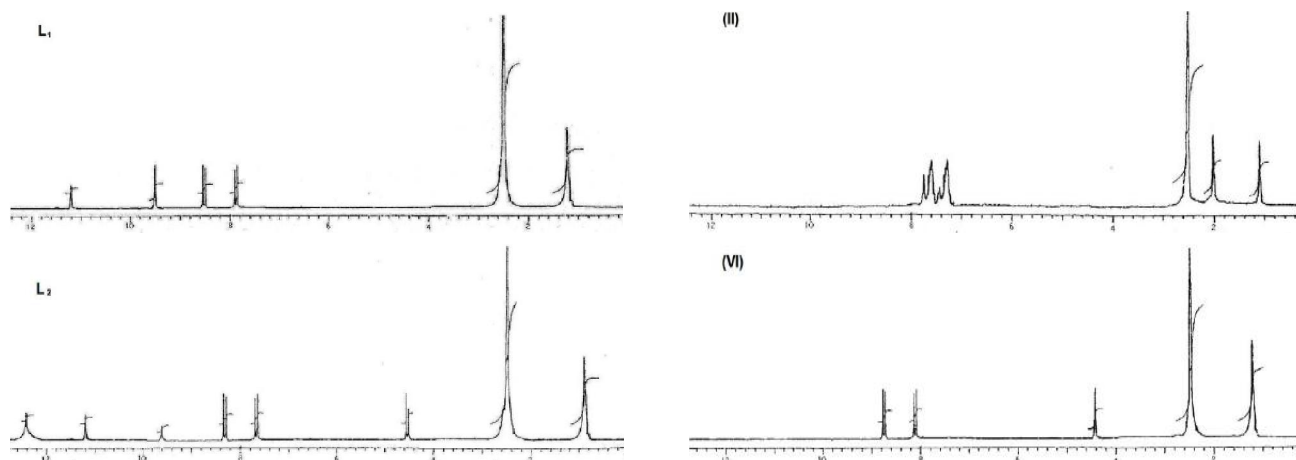


Figure 3 : The ¹H-NMR spectra of L₁, L₂, [NiL₁(H₂O)₂](Cl)₂·2H₂O (II) and [CuL₂(H₂O)₄]Cl (VI) complexes

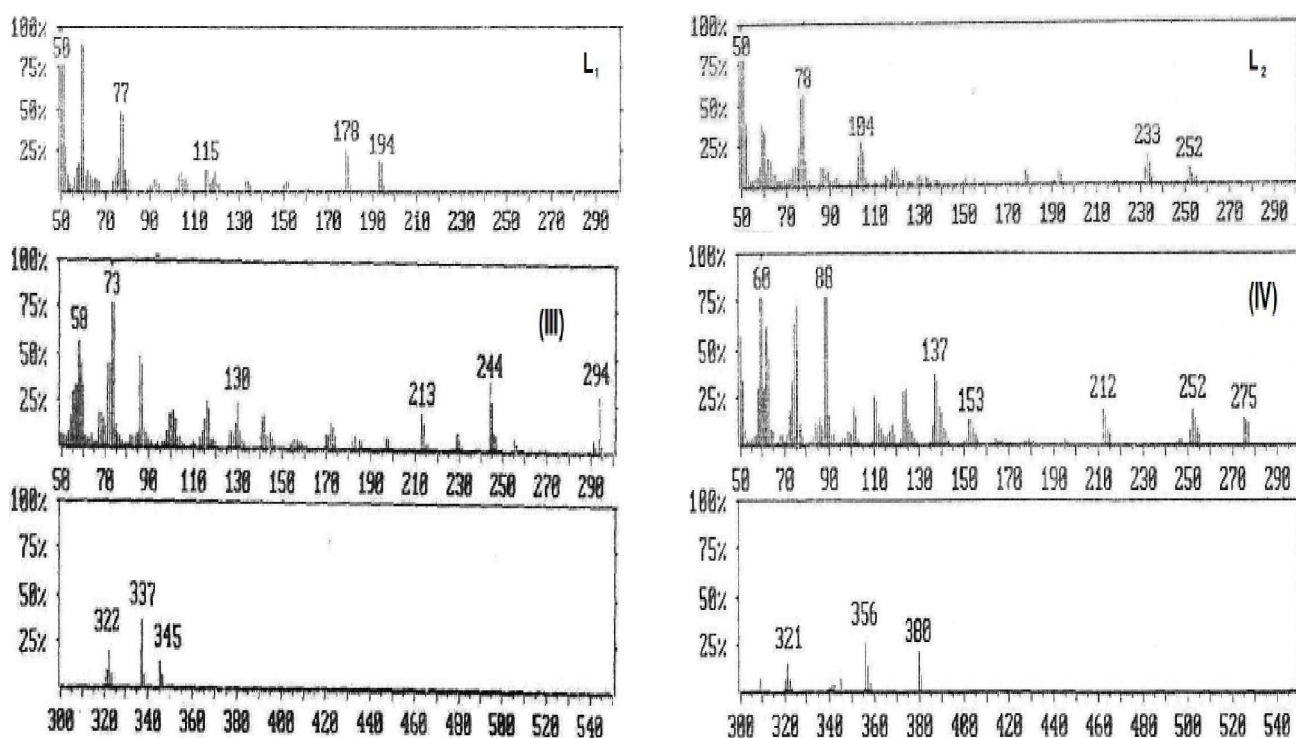


Figure 4 : The mass spectra L₁, L₂, [CuL₁(H₂O)](Cl)₂ (III) and [CoL₂(H₂O)₂]Cl (IV)

plexes, states that the hydrogen ion in the ligand molecule is substituted by the metal ions^[7]. The stretching asymmetric (ν_{as}) of carboxylate group between 1500 and 1542 cm^{-1} and of the symmetric vibrations (ν_s) at 1409-1403 cm^{-1} confirm these hypotheses. The shifting of $\nu(\text{C}=\text{N})$ in the spectra of the complexes indicate the sharing of this group in the formation of the complexes^[8]. The coordination of the metal ions via nitrogen atom is confirmed by presence the $\nu(\text{M}-\text{N})$ bands at range 430-493 cm^{-1} .

Electronic absorption spectra

The spectra of the two ligands and their complexes

in DMSO are shown in figure 2 and the spectral data are listed in TABLE 3.

There are two detected absorption bands in the spectra of the free ligands and their complexes, the first one which appears at range 205-260nm was assigned to $\pi-\pi^*$ ^[9], and the second which appears at range 285-385nm was assigned to $n-\pi^*$ intraligand transitions^[10,11]. These transitions also found in the spectra of the complexes, but they are shifted. There are evident that the increasing in the absorbance (hyperchromic effect) clarified in all of the spectra of the complexes attributed to the complexation behavior of two ligands

Full Paper

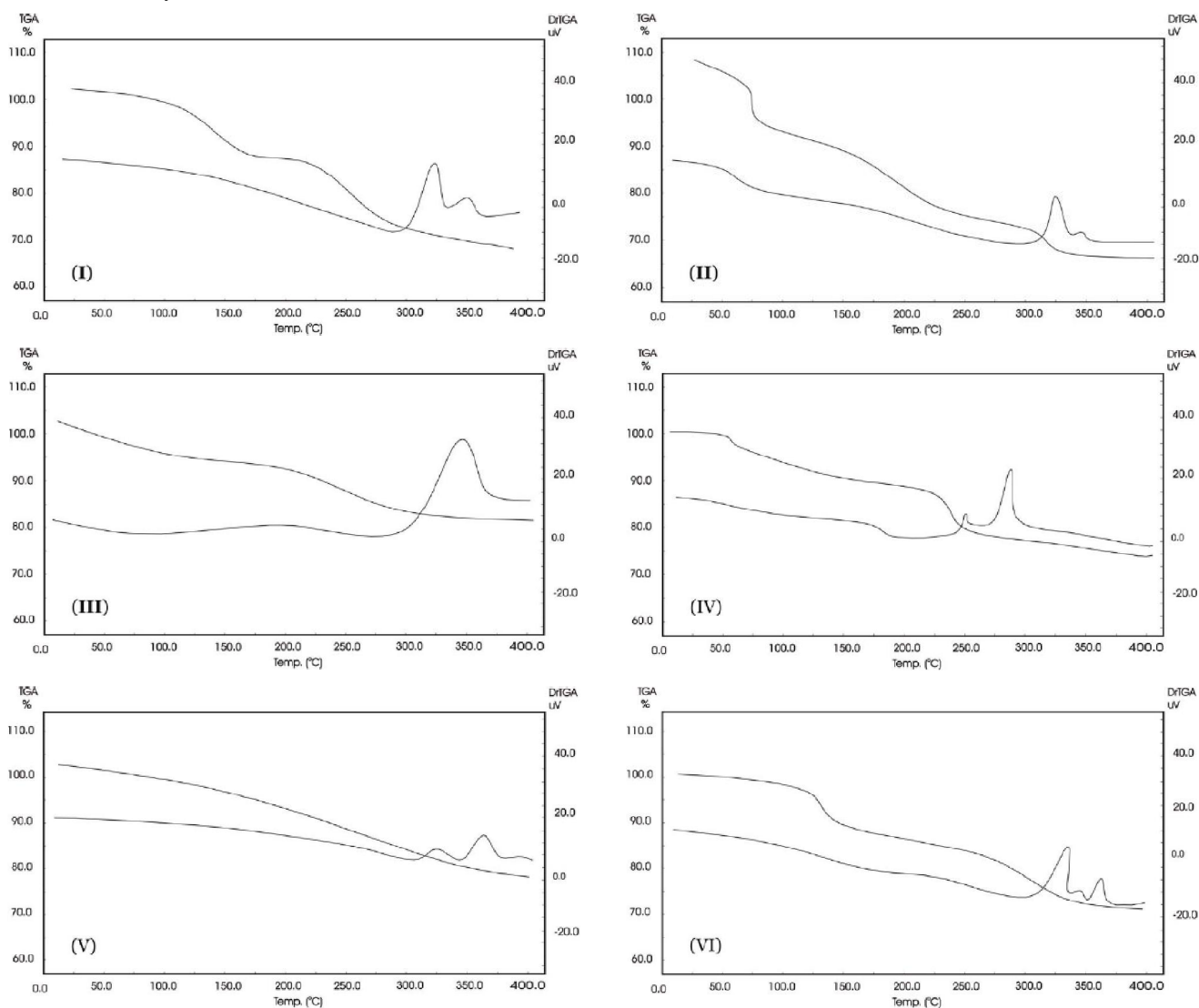


Figure 5 : The TG and DTG curves of the (I-VI) complexes

towards metal ions, confirming the coordination of the ligands to the metallic ions. The absorption bands at 448nm in the spectrum of $[\text{NiL}_2(\text{H}_2\text{O})_4]\text{Cl}_2 \cdot 2\text{H}_2\text{O}$ which can be attributed to ligand to metal charge-transfer.

$^1\text{H-NMR}$ spectra

The proton magnetic resonance spectra of the L_1 , L_2 , $[\text{NiL}_1(\text{H}_2\text{O})_2]\text{Cl}_2 \cdot 2\text{H}_2\text{O}$ (II) and $[\text{CuL}_2(\text{H}_2\text{O})_4]\text{Cl}$ (VI) complexes were analyzed (Figure 3).

The signals exhibited by the free ligand L_1 due to the NH group and NH_2 group protons at 9.57ppm and 11.25ppm, respectively, have been disappeared and only one signal is appeared in the spectrum of the $[\text{NiL}_1(\text{H}_2\text{O})_2](\text{Cl})_2 \cdot 2\text{H}_2\text{O}$ (II) complex at 2.11 ppm indicating the coordination of the two nitrogen atoms with the metal ion. Also, the signals exhibited by the free

ligand L_2 due to the NH group and carboxylate group protons at 9.57ppm and 12.42ppm, respectively, disappears in the spectrum of the $[\text{CuL}_2(\text{H}_2\text{O})_4]\text{Cl}$ (VI) complex indicating the coordination of nitrogen atom of NH group and oxygen atom (carboxylate ion) with the metal ion^[12,13]. The aromatic signals of pyridine ring do not shift significantly, thus showing that the magnetic environment of the aromatic ring has not changed significantly with coordination.

Mass spectra

The purity of L_1 , L_2 , $[\text{CuL}_1(\text{H}_2\text{O})_2]\text{Cl}_2$ (III) and $[\text{CoL}_2(\text{H}_2\text{O})_2]\text{Cl}$ (IV) was checked from mass spectra (Figure 4), where the spectra showed that a clearly base peaks (m/e) molecular weights and the intensity (%). The fragmentations of them are presented in Schemes

TABLE 6 : Antibacterial and antifungal activity data of L₁ and L₂ and their complexes (I-VI)

Compd. No.	Antibacterial activity data					Antifungal activity data	
	Gram positive bacteria			Gram negative bacteria		<i>Aspergillus Nigraer</i>	<i>Penicillium Sp.</i>
	<i>Bacillus Subtilis</i>	<i>Streptococcus Penumonia</i>	<i>Staphylococcus Aureas</i>	<i>E.Coli</i>	<i>Pesudomonas Sp.</i>		
L1	+++	+	-	-	+	++	++
L2	+	+	+++	+	-	+++	+
I	+++	++	-	+	++	++	+++
II	+++	+++	+	++	++	+++	+++
III	+++	+	+	-	+	++	++
IV	+++	+	+++	+	++	+++	+
V	++	+++	+++	+++	++	+++	+++
VI	+	+++	+++	+	+	+++	+

1-4. Their is difference between the fragmentation path way of the two ligand rather than the two complexes resulted according to the place of complexation, the formation of the complexes via NH and NH₂ groups incase of L₁ and via NH and COOH groups in L₂.

Thermogravimetric analysis

Thermal analysis curves (TG and DTG) of the studies complexes are shown in figure 5. The thermoanalytical results are summarized in TABLE 4.

[CoL₁(H₂O)₂]Cl₂ (I)

The thermal decomposition of this complex occurs at two steps. The first degradation step take place in the range of 25-250°C and it corresponds to the eliminated of the pyridine ring due to a weight loss of 21.85% in a good matching with theoretical value 22.82%. The second step fall in the range of 250-400°C which is assigned to loss of C₃H₈N₃OS (organic rest) with a weight loss 39.28% and the calculated value is 39.19%.

[NiL₁(H₂O)₂]Cl₂.2H₂O (II)

The thermal decomposition of [NiL₁(H₂O)₂]Cl₂.2H₂O complex completely in three steps. The first degradation step take place in the range of 25-100°C and it is corresponds to the eliminated of four water molecule due to a weight loss of 17.83% in a good matching with theoretical value 18.19%. The second step fall in the range of 100-225°C which is assigned to loss of the pyridine ring with a weight loss 19.86% and the calculated value is 19.72%. The third step fall in the range of 225-400°C which is assigned to loss of C₃H₆N₃S (organic rest) with a weight loss 29.52% and the calculated value is 29.32%.

[CuL₁(H₂O)₂]Cl₂ (III)

The Cu(II) complex decomposed like Co(II) complex only in two steps. The first extended from 25°C to 200°C and can be assigned to the loss of pyridine ring, representing a weight loss of 22.53% and its calculated value is 22.52%. The second step occurring at 200-400°C corresponding to the loss of C₃H₈N₃OS (organic moiety), representing a weight loss of 39.29% and its calculated value is 38.67%.

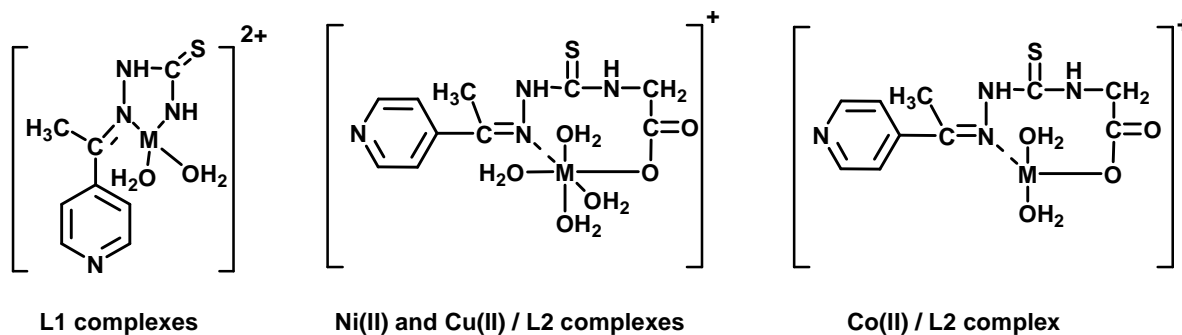
[CoL₂(H₂O)₂]Cl (IV)

This complex decomposed also in two steps, the first one occurring at 25-100°C and corresponding to the evolution of all two coordination water molecules, representing a weight loss of 9.51% and its calculated value is 9.43%. The second step occurring at 100-400°C is corresponding to the loss of C₁₀H₁₁N₄OS (organic rest), representing a weight loss of 60.05% and its calculated value is 61.61%.

[NiL₂(H₂O)₄]Cl.2H₂O (V)

To make sure about the proposed formula and structure for the new Ni(II) complex, [NiL₂(H₂O)₄]Cl.2H₂O (V), thermo gravimetric (TG) and differential thermo gravimetric analysis (DTG) was carried out for this complex under N₂ flow. DTG thermogram is shown in figure 4. The thermal decomposition of the (V) complex proceeds approximately with main two degradation steps. The first stage occurs at maximum temperature of 65°C. The weight loss associated with this stage 23.51% which is very close to the theoretical value of 23.83% corresponding to the loss of six water molecules as will be described in TABLE 4. The second

Full Paper

Scheme 5 : The structures L_1 and L_2 complexes

step occurring at 225–400°C is corresponding to the loss of $C_{10}H_{11}N_4OS$ (organic moiety), representing a weight loss of 10.07% and its calculated value is 9.87%. The final product resulted at 400°C was NiO.

[CuL₂(H₂O)₄]Cl (VI)

As mentioned above in the Co(II) and Ni(II) complexes, [CuL₂(H₂O)₄]Cl (VI) complex, also has two decomposition steps. The first step located in the range between 25–150°C at maximum temperature DTG_{max} = 115°C and the weight loss at this step is 12.52% due to the loss of three water molecules, in agreement with the theoretical weight loss value of 12.79%. The second step occurring at 150–400°C is corresponding to the loss of the last water molecule and $C_{10}H_{11}N_4OS$ (organic moiety), representing a weight loss of 59.79% and its calculated value is 59.95%. The final formed product at 400°C is CuO.

Kinetic studies

In recent years there has been increasing interest in determining the rate-dependent parameters of solid-state non-isothermal decomposition reactions by analysis of TG curves. Several equations^[9-21] have been proposed as means of analyzing a TG curve and obtaining values for kinetic parameters. Many authors^[14-19] have discussed the advantages of this method over the conventional isothermal method. The rate of a decomposition process can be described as the product of two separate functions of temperature and conversion^[15], using

$$d\alpha/dt = k(T)f(\alpha) \quad (1)$$

where α is the fraction decomposed at time t , $k(T)$ is the temperature dependent function and $f(\alpha)$ is the conversion function dependent on the mechanism of decomposition. It has been established that the tempera-

ture dependent function $k(T)$ is of the Arrhenius type and can be considered as the rate constant k .

$$k = A e^{-E^*/RT} \quad (2)$$

where R is the gas constant in (Jmol⁻¹K⁻¹). Substituting equation (2) into equation (1), we get,

$$d\alpha/dT = (A/\phi e^{-E^*/RT})f(\alpha)$$

where ϕ is the linear heating rate dT/dt . On integration and approximation, this equation can be obtained in the following form

$$\ln g(\alpha) = -E^*/RT + \ln[AR/\phi E^*]$$

where $g(\alpha)$ is a function of α dependent on the mechanism of the reaction. The integral on the right hand side is known as temperature integral and has no closed for solution. So, several techniques have been used for the evaluation of temperature integral. Most commonly used methods for this purpose are the differential method of Freeman and Carroll^[14] integral method of Coat and Redfern^[16], the approximation method of Horowitz and Metzger^[19].

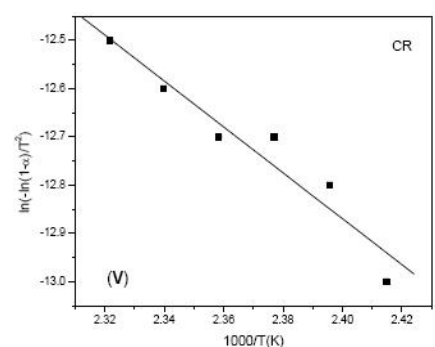
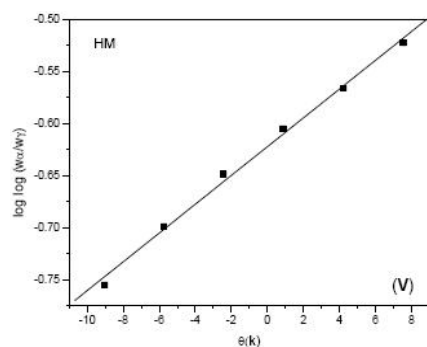
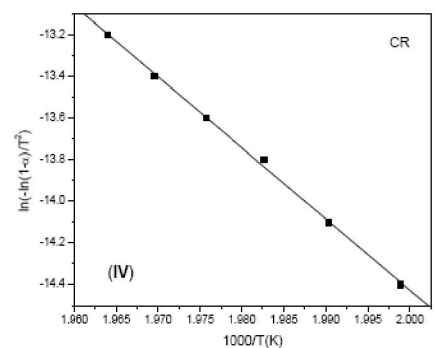
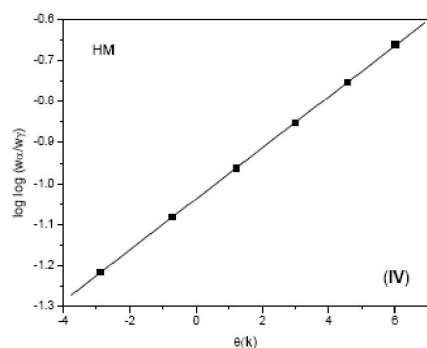
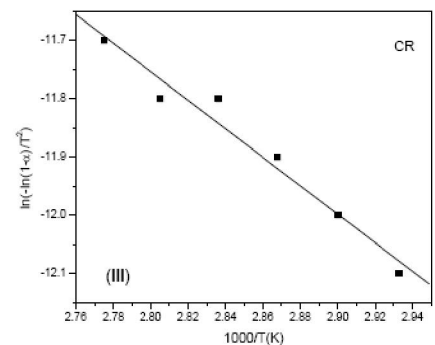
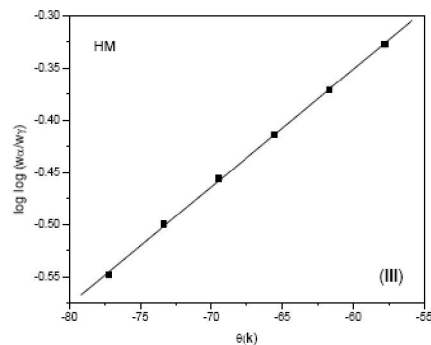
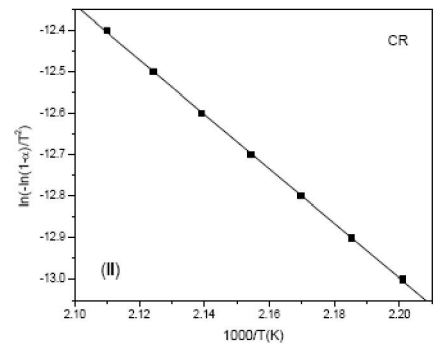
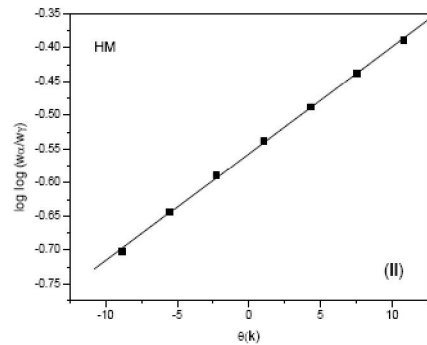
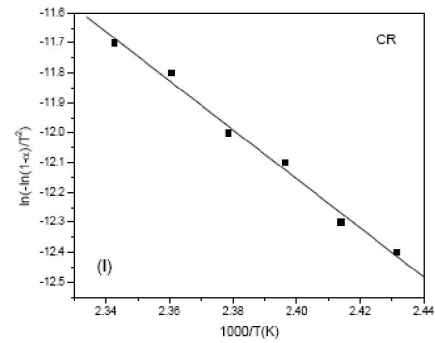
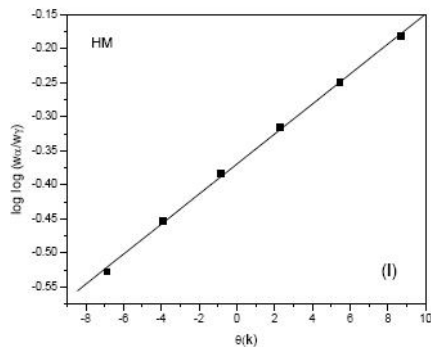
In the present investigation, the general thermal behaviors of the L_1 and L_2 complexes in terms of stability ranges, peak temperatures and values of kinetic parameters, are shown in figure 6 and TABLE 5. The kinetic parameters have been evaluated using the following methods and the results obtained by these methods are well agreement with each other. The following two methods are discussed in brief.

Coats- redfern equation

The Coats-Redfern equation, which is a typical integral method, can be represented as:

$$\int_0^\alpha \frac{d\alpha}{(1-\alpha)^n} = \frac{A}{\phi} \int_{T_1}^{T_2} \exp\left(-\frac{E^*}{RT}\right) dt$$

For convenience of integration the lower limit T_1 is



Full Paper

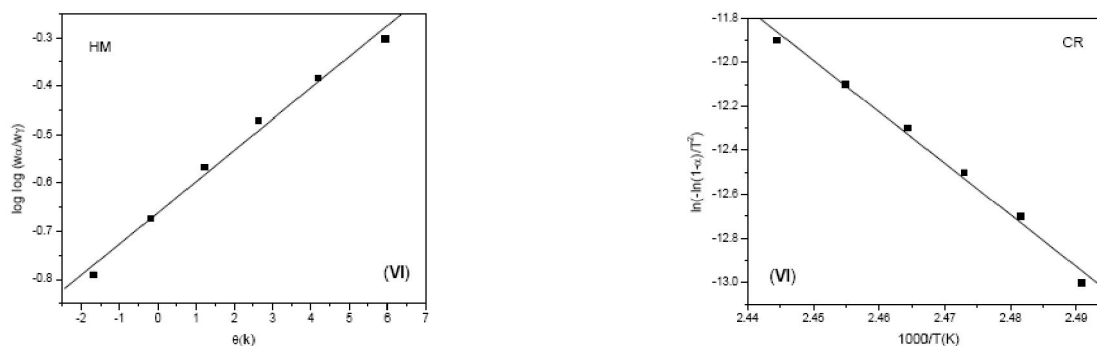


Figure 6 : Horowitz–Metzger (HM), Coats–Redfern (CR) of the first step of the L_1 and L_2 complexes

usually taken as zero. This equation on integration gives;

$$\ln\left[-\frac{\ln(1-\alpha)}{T^2}\right] = -\frac{E^*}{RT} + \ln\left[\frac{AR}{\phi E^*}\right]$$

A plot of left-hand side (LHS) against $1/T$ was drawn. E^* is the energy of activation in J mol^{-1} and calculated from the slop and A in (s^{-1}) from the intercept value. The entropy of activation ΔS^* in $(\text{JK}^{-1}\text{mol}^{-1})$ was calculated by using the equation:

$$\Delta S^* = R \ln(Ah/k_B T_s) \quad (3)$$

where k_B is the Boltzmann constant, h is the Plank's constant and T_s is the DTG peak temperature^[22].

Horowitz-Metzger equation

The Horowitz-Metzger equation is an illustrative of the approximation methods. These authors derived the relation:

$$\log\left[\frac{1-(1-\alpha)^{1-n}}{1-n}\right] = E^*\theta/2.303RT_s^2 \text{ for } n \neq 1 \quad (4)$$

When $n = 1$, the LHS of equation 4 would be $\log[-\log(1-\alpha)]$. For a first-order kinetic process the Horowitz-Metzger equation may be written in the form:

$$\log[\log(w_\alpha/w_\gamma)] = E^*\theta/2.303RT_s^2 - \log 2.303$$

where $\theta = T - T_s$, $w_\gamma = w_\alpha - w$, $w_\alpha =$ mass loss at the completion of the reaction; $w =$ mass loss up to time t . The plot of $\log[\log(w_\alpha/w_\gamma)]$ vs θ was drawn and found to be linear from the slope of which E^* was calculated. The pre-exponential factor, A , was calculated from the equation:

$$E^*/RT_s^2 = A/\phi \exp(-E^*/RT_s)$$

The entropy of activation, ΔS^* , was calculated from equation 3. The enthalpy activation, ΔH^* , and Gibbs free energy, ΔG^* , were calculated from; $\Delta H^* = E^* - RT$ and $\Delta G^* = \Delta H^* - T\Delta S^*$, respectively.

The reaction for which ΔG is positive and ΔS is negative considered as unfavorable or non spontane-

ous reactions.

Reactions are classified as either exothermic ($\Delta H < 0$) or endothermic ($\Delta H > 0$) on the basis of whether they give off or absorb heat. Reactions can also be classified as exergonic ($\Delta G < 0$) or endergonic ($\Delta G > 0$) on the basis of whether the free energy of the system decreases or increases during the reaction.

The thermodynamic data obtained with the two methods are in harmony with each other. The correlation coefficients of the Arrhenius plots of the thermal decomposition steps were found to lie in the range 0.9630 to 0.9999, showing a good fit with linear function. It is clear that the thermal decomposition process of all L_1 and L_2 complexes is non-spontaneous, i.e, the complexes are thermally stable.

Microbiological screening

The results of antibacterial activities in vitro of the two ligands and their complexes are given in TABLE 6. From the results we can see that all the effect on the selected bacteria can be ordered as, *Bacillus Subtilis* > *Streptococcus Penumonia* > *Staphylococcus aureus* > *Escherichia Coli* > *Pesudomonas Sp.*

Also the two ligands and their complexes have been evaluated for their antifungal activity. The minimal inhibitory concentration values listed in TABLE 6 show that all the test compounds have more effect on *Aspergillus Nigraer* than *Penicillium Sp.*

Structure of the L_1 and L_2 and their complexes

The fact that these compounds were isolated as powders and not as single crystals means that no complete structure determination can be made. Accordingly, the above mentioned discussions using elemental analysis, molar conductance, (infrared, $^1\text{H-NMR}$ and mass) spectra as well as thermogravimetric analysis; the sug-

gested structures of the L_1 and L_2 and their complexes can be represented in Scheme 5.

REFERENCES

- [1] A.Baxter, C.Bennion, J.Bent, K.Boden, S.Brough, A.Cooper, E.Kinchin, N.Kindon, T.McInally, M.Mortimore, B.Roberts, J.Unitt; *Bio.Med. Chem.Lett.*, **13**, 2625 (2003).
- [2] Farhanullah, D.Sil, B.K.Tripathi, A.K.Srivastava, V.J.Ram; *Bio.Med.Chem.Lett.*, **14**, 2571 (2004).
- [3] B.T.Khan, K.Najmuddin, S.Shamsuddin, S.M.Zakeeruddin; *Inorg.Chim.Acta*, **709**, 129 (1990).
- [4] B.T.Khan, K.Venkatasubramanian, K.Najmuddin, S.Shamsuddin, S.M.Zakeeruddin; *Inorg.Chim.Acta*, **179**, 117 (1991).
- [5] F.D.Popp, H.Pajouhesh; *J.Pharma.Sci.*, **17**, 1052 (1988).
- [6] M.S.Refat; *J.Mol.Struct.*, Under Press, (2007).
- [7] M.S.Refat, A.Sabry El-Korashy, Deo Nandan Kumarc, S.Ahmed Ahmed; *Spectrochimica Acta Part A*, Under Press, (2007).
- [8] M.S.Refat, A.A.Ibrahim; *Spectrochimica Acta Part A*, Under Press, (2007).
- [9] W.Barnum; *J.Inorg.Nucl.Chem.*, **21**, 221 (1961).
- [10] R.H.Holm, F.A.Cotton; *J.Am.Chem.Soc.*, **80**, 5658 (1958).
- [11] F.A.Cotton, C.W.Wilkinson; 'Advanced Inorganic Chemistry', 3rd Ed., Interscience Publisher, New York, (1972).
- [12] R.Roy, M.C.Saha, P.S.Roy; *Trans.Met.Chem.*, **5110**, 51 (1990).
- [13] P.P.Carbi, F.Cagnim, L.P.B.Sabeh, A.C.Massabni, C.M.Costa-Neto; *Spectrochim. Acta Part A*, In Press, (2006).
- [14] E.S.Freeman, B.Carroll; *J.Phys.Chem.*, **62**, 394 (1958).
- [15] J.Sestak, V.Satava, W.W.Wendlandt; *Thermochem.Acta*, **7**, 333 (1973).
- [16] A.W.Coats, J.P.Redfern; *Nature*, **201**, 68 (1964).
- [17] T.Ozawa; *Bull.Chem.Soc.Jpn.*, **38**, 1881 (1965).
- [18] W.W.Wendlandt; 'Thermal Methods of Analysis', Wiley, New York, (1974).
- [19] H.W.Horowitz, G.Metzger; *Anal.Chem.*, **35**, 1464 (1963).
- [20] J.H.Flynn, L.A.Wall; *Polym.Lett.*, **4**, 323 (1966).
- [21] P.Kofstad; *Nature*, **179**, 1362 (1957).
- [22] J.H.F.Flynn, L.A.Wall; *J.Res.Natl.Bur.Stand.A*, **70**, 487 (1996).